

Magnetic frustration in mixed valence manganites

J. L. García-Muñoz, J. Fontcuberta, B. Martínez, A. Seffar, S. Piñol, and X. Obradors
*Institut de Ciència de Materials de Barcelona, Consejo Superior de Investigaciones Científicas,
 Campus Universitat Autònoma de Barcelona, Bellaterra 08193, Catalunya, Spain*

(Received 9 September 1996)

Investigation of structural and magnetotransport properties of $L_{2/3}A_{1/3}\text{MnO}_3$ ($A=\text{Ca},\text{Sr}$) oxides reveals a gradual increase of the magnetic frustration with bending of the Mn-O-Mn bonds. The relative strength of competing magnetic interactions is controlled not only by R_0 [R_0 is the mean radius of the ions at the (L, A) site] but also by the electronegativity of the divalent cation. The magnetoresistance of these oxides results mainly from spin disorder and the narrowing of the $\sigma(e_g)$ band has only a minor effect. We have observed that the curve $T_C(R_0)$ is not universal but it is sensitive to the alkaline ions. [S0163-1829(97)51402-0]

The discovery of colossal magnetoresistive effects (CMR) in ferromagnetic manganese perovskites (with a magnetoresistance greater than (10⁷%) (Ref. 1) is attracting much interest due to the importance of their potential technological applications and the fascinating physics involved. It is widely accepted that strong magnetostructural and electronic correlation effects are at the origin of the exceptional physical properties of this family of materials. In the framework of the double-exchange interaction model (DE) (Ref. 2) the mobile charge carriers in the substituted $L_{1-x}A_x\text{MnO}_3$ (L , lanthanide; A , divalent cation) compounds mediate the ferromagnetic interactions between $\text{Mn}^{3+/4+}$ ions. The ferromagnetic Curie temperature (T_C) is related to the Hund's coupling (J_H) between the core spins ($S=3/2$, Mn t_{2g}^3 electrons) and mobile e_g electrons ($S=1/2$), and to the strength of the hopping integral t_σ^F between $e_g(\text{Mn})-2p_\sigma(\text{O})-e_g(\text{Mn})$ orbitals, which controls at the same time the electronic conductivity. Nevertheless ferromagnetism (F) coexists with antiferromagnetic (AF) exchange interactions between the localized t_{2g} spins [$t_{2g}(\text{Mn})-2p_\pi(\text{O})-t_{2g}(\text{Mn})$] that are governed by the transfer integral t_π^{AF} . In this complex picture, the first step in the race for technological applications is the identification of the relevant physical factors governing the CMR in order to tailor its response in the most appropriate way. Up to now, electrical and magnetic data^{3,4} reveal that the CMR response and the Curie temperature T_C strongly depend on the radius of the lanthanide (R_0) in the $L_{1-x}A_x\text{MnO}_3$ family having fixed the hole content to the optimal value $x \approx 1/3$. The structural tuning of CMR by varying R_0 has been proposed to be the result of changes in the Mn-O-Mn bond angle^{3,4} that modify the Mn-Mn hopping of e_g electrons.

Here we present experimental data on the series $L_{2/3}A_{1/3}\text{MnO}_3$ with $A=\text{Ca}$ and Sr which reveal a gradual increase of the magnetic frustration as the Mn-O-Mn bond bends. The existence of differences in the electrical and magnetic behavior of Sr and Ca specimens having identical distortion (same Mn-O-Mn bond bending) and doping is clearly evidenced. They are triggered by differences in the covalent component of the A-O bonds, making evident that electronic effects, apart from bond bending, also play a role in modifying T_C in $L_{2/3}A_{1/3}\text{MnO}_3$ oxides.

The polycrystalline $(L,L')_{2/3}A_{1/3}\text{MnO}_3$ specimens ($L,L'=\text{Nd}, \text{Pr}, \text{Y}, \text{La}$; $A=\text{Ca}, \text{Sr}$) were synthesized by the solid-

state reaction method, mixing stoichiometric amounts of the appropriate high-purity oxides at 1100 °C (two sinterings) and 1400 °C (one sintering) with several pressings and grindings after each sinterization process under O₂. Neutron-diffraction data were obtained at the Reactor Orphée of the Laboratory Léon-Brillouin. 3T2 and G4.1 powder diffractometers ($\lambda=1.226$ and 2.426 Å) were used between 1 K and room temperature. All the samples were single phase with no detectable secondary phases. Cationic stoichiometry was determined to be the nominal (± 0.01) by neutron-diffraction analysis. The oxygen contents were found to be 3.00 within the calculated standard error (1%). Magnetization measurements were performed by using a superconducting quantum interference device magnetometer. The Curie temperatures determined from neutron, magnetic, and resistivity measurements confirm the strong dependence of T_C on R_0 [the average radius of the ions at the (L, A) site] or, equivalently, on the tolerance factor t [defined as $t=(R_0+R_{[\text{O}]})/\sqrt{2}(R_{[\text{Mn}]}+R_{[\text{O}]})$]. The structural details have been thoroughly investigated. In order to separate the different variables of the problem, we will address first the main interatomic distances and angles that determine the $p-d$ hybridization. We will show that, in spite of the changes in T_C and the strong variation of $\Delta R/R(\%)$, the average Mn to O distance is not significantly modified for a fixed hole concentration of 1/3. In Fig. 1 we represent the average Mn-O distance of several samples with very different mean-ionic radii R_0 , as obtained from high-resolution neutron-diffraction measurements. According to these results the mean Mn-O distance is $\langle d_{\text{Mn-O}} \rangle \approx 1.960(2)$ Å in the series.

Both the $d_{\text{Mn-O}}$ distance and the Mn-O-Mn bond angle are the basic structural parameters controlling the hybridization strength between Mn $3d$ and O $2p$ states (t_σ^F and t_π^{AF}). In the $Pbnm$ symmetry [samples with $t < \approx 0.93$ (Ref. 3)] there are two Mn-O-Mn bond angles, while for $R-3C$ ($t > \approx 0.93$) there is only one. We show in Fig. 1(b) that the mean value $\theta = \langle \text{Mn-O-Mn} \rangle$ subtended in $L_{2/3}A_{1/3}\text{MnO}_3$ ($L_{0.7}A_{0.3}\text{MnO}_3$ data are taken from Ref. 4) monotonically increases with rising t , or equivalently, the ionic radius R_0 (values from Ref. 5 have been used). Therefore, after Fig. 1, we are led to conclude that the essential structural feature responsible for the observed T_C dependence on t is the mean ionic radius R_0 and, more specifically speaking, the tilting of the MnO_6 octahedra, with origin at the free space left in the structure by

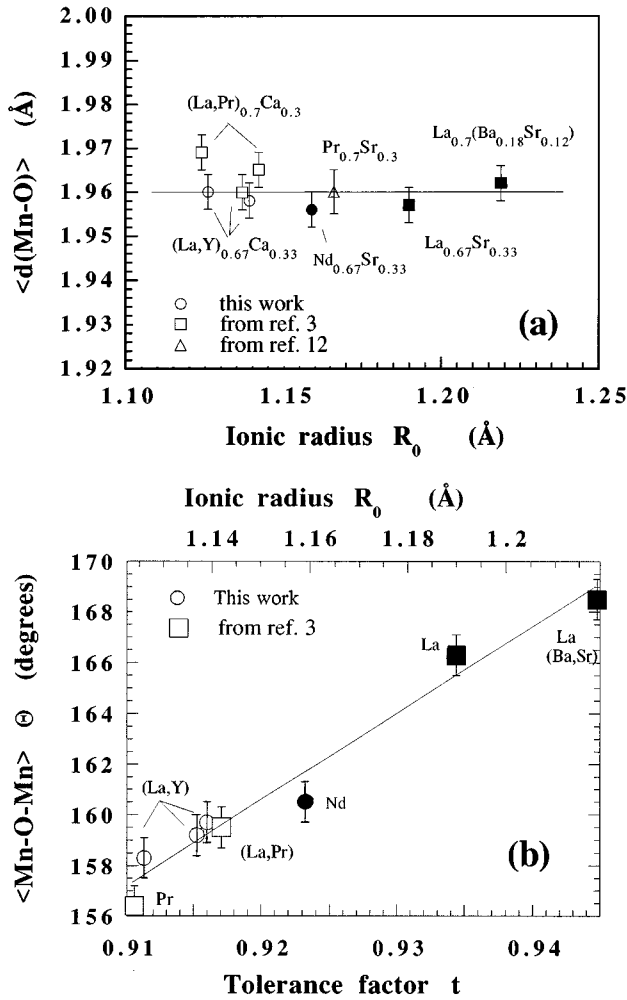


FIG. 1. (a) Average Mn-O distance in the MnO_6 octahedra of the $L_{1-x}A_x\text{MnO}_3$ ($x=0.3$ and 0.33) family of magnetoresistive manganites as a function of the mean (L , A) radii R_0 . Empty and filled symbols correspond respectively to Ca and Sr samples. Circles correspond to samples measured in this work. (b) Average Mn-O-Mn angle (θ) as a function of tolerance factor t (both defined in the text) in the same family of perovskites. Empty and filled symbols correspond respectively to Ca and Sr samples.

small L ions. It is worth mentioning that $\theta(t)$ is a unique function of t , irrespective of the divalent (Sr^{2+} or Ca^{2+}) alkaline used. The evolution of $\theta(t)$ depicted in Fig. 1(b) is of capital importance since the essential physics in these materials is closely related to θ . The implications are twofold. On one side, the efficiency of the ferromagnetic double-exchange mechanism^{2,6,7} is tuned by the hopping term of the outer-shell d electrons (t_{σ}^F). Therefore, by increasing the hybridization between Mn e_g and O $2p$ orbitals, the mobility of the charge carriers and the mechanism of double-exchange are favored. Obviously, a reduction of θ implies a weaker $e_g-2p_{\sigma}-e_g$ overlapping and a narrower bandwidth (W). On the other side, an increase of the electron-phonon coupling, arising from the dynamic Jahn-Teller splitting of the e_g Mn orbitals, is expected when the bandwidth becomes narrower.⁸

Further insight may be gained by analyzing the effects of the structural distortion on the magnetic properties. The gradual loosening of collinearity of the overall magnetic order is demonstrated in Fig. 2(a) where we plot the zero-field

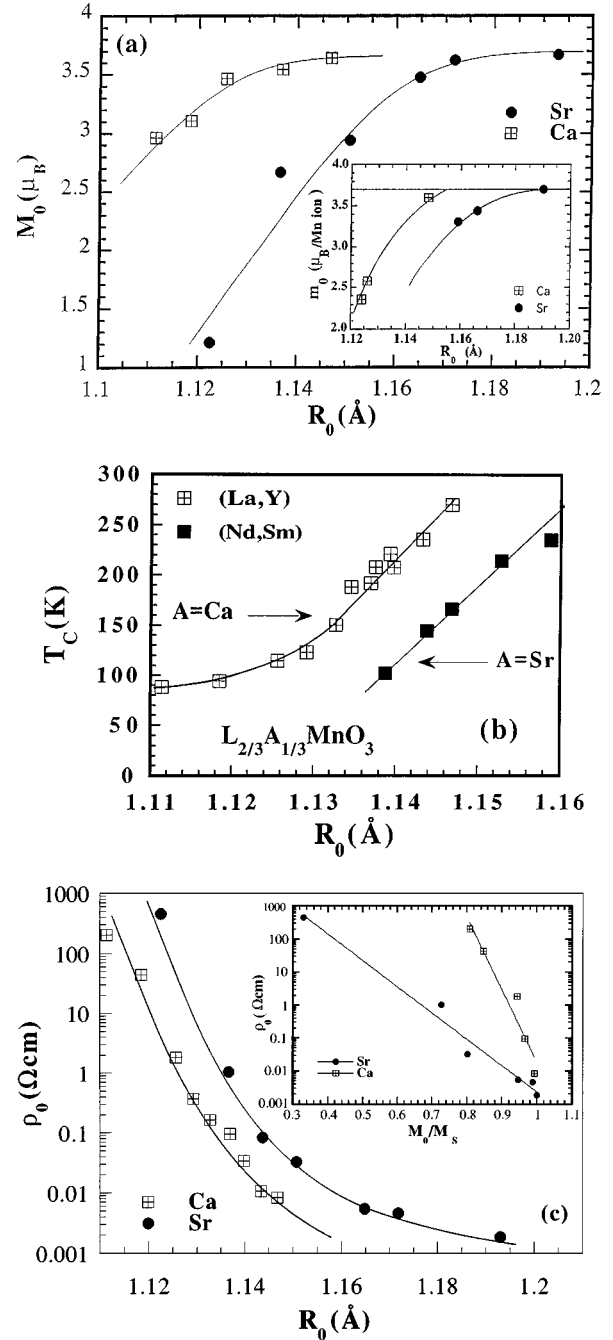


FIG. 2. (a) Dependence of the zero-field extrapolated saturation magnetization vs R_0 for $\text{La}_{2/3-x}\text{Y}_x\text{A}_{1/3}\text{MnO}_3$ [$x=0, 0.07, 0.10, 0.15, 0.20$ ($A=\text{Ca}$) and $x=0, 0.07, 0.10, 0.15, 0.20, 0.25$ ($A=\text{Sr}$)]. The inset shows the dependence on R_0 of the total ordered Mn moment at 1.5 K (m_0 , from neutron diffraction) of some Sr and Ca samples. (b) Curie temperatures (T_C) vs R_0 for the series of manganites ($L_{1-x}L'_x)_{2/3}A_{1/3}\text{MnO}_3$, $A=\text{Ca}$ [$L'=\text{Y}$ ($0 \leq x \leq 0.25$), $L'=\text{Yb, Gd, Dy}$ ($x=0.07$)] and $A=\text{Sr}$ [$L'=\text{Y}$ ($0 \leq x \leq 0.25$)] obtained from magnetic measurements ($H=25$ Oe) and electrical resistivity ($H=0$) (while cooling). (c) Residual resistivity vs the averaged lanthanide radius R_0 for the same set of samples [$A=\text{Ca}$, $L'=\text{Y}$ ($0 \leq x \leq 0.25$), and $A=\text{Sr}$ $L'=\text{Y}$ ($0 \leq x \leq 0.5$)] The inset shows the residual resistivity vs the reduced magnetization M_0/M_S .

extrapolated saturation magnetization M_0 (at 5 K) as a function of R_0 for the series $(La_{1-x}Y_x)_{2/3}A_{1/3}MnO_3$ with $A = Ca$ and Sr . The observation of a decrease in M_0 when reducing R_0 , that is when the bond bending increases, means that antiferromagnetic interactions compete with ferromagnetism. This fact is also confirmed by the observed reduction of T_C . Then, it can be concluded that varying θ modifies both the t_σ^F and t_π^{AF} integrals, but at a different rate, thus changing the $|J_{AF}|/|J_F|$ ratio.

Even more, the neutron-diffraction data show [inset of Fig. 2(a)] that the ordered magnetic component of Mn moments is progressively reduced as R_0 is shortened; thus indicating that the nonferromagnetic spin components are essentially disordered. Consequently it is clear that the softening of the F interactions, relative to the AF term, gradually leads to a more disordered magnetic structure. This F-AF competition generates some degree of frustration leading to the appearance of a spin glasslike phase, whose typical magnetic behavior has been recently observed⁹ for smaller R_0 , when the metalliclike behavior is lost.

It is interesting to note that, in addition, our data of Fig. 2(a) also reveal an unexpected dependence of the reduction of $M_0(R_0)$ on the divalent alkaline. It turns out that for similar R_0 values, M_0 is remarkably smaller for Sr-doped manganites than for the Ca-doped ones. Since neutron-diffraction analysis reveals that both series are stoichiometry indistinguishable, this observation indicates that the strength and competition of the AF/F interactions is also influenced by the nature of divalent alkalines. We believe that the distinct electron affinity in the A-O bond underlies the observed differences. According to this, the data of Fig. 2(a), which suggest weaker ferromagnetic coupling for Sr-based oxides, also predict that the Curie temperature (T_C) should be smaller than in similarly distorted Ca-based oxides. This prediction is clearly confirmed in Fig. 2(b), where we show T_C vs R_0 for $(L_{1-x}L'_x)_{2/3}A_{1/3}MnO_3$ ($A = Ca$ and Sr). These results are in clear contrast with earlier suggestions indicating that T_C was simply triggered by steric effects. Consequently, a universal curve $T_C(R_0)$ should not exist since the alkaline ions play also a role.

At this point, it is useful to recall that the s and p orbitals of the A^{2+} cations compete directly with the Mn t_{2g} orbitals for the O:2 p_π electrons.¹⁰ That is, the O:2 p_π electrons are simultaneously shared by the Mn: t_{2g} orbitals, with which they are π bonded, and the outer A orbitals, with which they are σ bonded. Therefore, the presence of a more electropositive alkaline ion (Sr) makes the covalent overlap of the A^{2+} -O bond smaller, and increases the $t_{2g}(\text{Mn})$ -2 $p_\pi(\text{O})$ - $t_{2g}(\text{Mn})$ hybridization (t_π^{AF}), which is at the origin of the antiferromagnetism in this system. Thus, for a given bond distortion θ : $t_\pi^{AF}(\text{Sr}) > t_\pi^{AF}(\text{Ca})$, and the relative strength $|J_{AF}|/|J_F|$ is also bigger with Sr than with Ca. The above relative change implies that magnetic frustration is enhanced at the Sr series and so the effective ferromagnetic coupling and T_C decrease.

The subtle electronic effects produced by the alkalines also have observable consequences in transport data. In Fig. 2(c) it is shown how the zero-field residual resistivity ρ_0 is always higher, as a function of R_0 , in the Sr-doped samples compared to that of Ca samples for a similar distortion. The

displacement of the $\rho(R_0)$ curve is a signature of the different degree of spin disorder. The inset of Fig. 2(c), displaying ρ_0 vs M_0/M_s (M_s is the full $Mn^{3+/4+}$ ion magnetization), indicates that, as previously suggested by Coey *et al.*,¹¹ the residual resistivity is an exponential function of the ferromagnetic ordered component: $\rho_0 \approx \exp[-\beta(M_0/M_s)]$, where $\beta \approx 0.13$ and 0.52 for Sr and Ca, respectively. An exponential dependence $\rho \approx \exp(-t_\sigma^{\text{eff}})$ is also expected for a polaron hopping transport mechanism. Within the simplest DE model $t_\sigma^{\text{eff}} \approx t_\sigma^F \cos \Phi_{ij}$, where t_σ^F is the e_g -O- e_g overlap integral and Φ_{ij} , is the angle between neighboring localized spins. Since the spin-dependent contributions to the conductivity are already included in the (M_0/M_s) term, the parameter β must be mainly governed by the transfer integral t_σ^F (or W). However, it is straightforward to note that the experimental observation of the law $\rho_0 \approx \exp[-\beta(M_0/M_s)]$ indicates that spin disorder is clearly the source of scattering and that t_σ has a weaker dependence on R_0 than Φ_{ij} . Therefore, it follows that the colossal magnetoresistance of the mixed-valence manganites and its dependence on R_0 is mainly triggered by the spin arrangement resulting from the competing AF/F interactions between Mn ions. Bandwidth variations ($\approx \beta$) play only a secondary role on the overall magnetotransport properties.

Finally, our finding that $\beta(\text{Ca}) > \beta(\text{Sr})$ would indicate that the t_σ^F coupling is also sensitive to the nature of the alkaline ions. Although the exact origin of this difference is at present not clear, one could speculate that it signals a distinct bandwidth [$t_\sigma^F(\text{Ca}) > t_\sigma^F(\text{Sr})$] or a softer coupling for polarons ($\approx t_\sigma^F/\theta_D$) in the Sr case than in the Ca case.^{9,10} Further investigations of electronic structure and transport properties will be necessary to ascertain which is the dominant factor.

In summary, we have shown that steric and electronic factors control the competing magnetic interactions in mixed-valence manganites. The Mn-O-Mn bond bending weakens both the ferromagnetic and antiferromagnetic coupling, but at a different rate, raising the magnetic frustration and thus lowering T_C and increasing the residual resistivity. We have also demonstrated that for stoichiometric and equally doped $L_{2/3}A_{1/3}MnO_3$ manganites, $T_C(R_0)$ displays a different functional dependence for Sr and Ca doping. Despite θ being a unique function of t , the M-I transition temperatures are systematically lower with divalent Sr than Ca. In addition, for the same degree of distortion in the structure, the spin disorder is systematically smaller with Ca than with Sr. Such a different behavior of both series can be understood on the basis of the distinct electronegativity of the alkaline ions, a difference that is usually neglected. The existence of new electronic effects in addition to the known structural ones opens new possibilities in the control of the anomalous resistivity and the magnetoresistance of these ferromagnetic metals.

We would like to acknowledge financial support by the CICYT-MIDAS (MAT94-1924-CO2), DGICYT (PB92-0849) projects and the Generalitat de Catalunya (GRQ95-8029). A.S. is grateful to the Instituto de Cooperación con el Mundo Árabe for financial support. The L.L.B. is acknowledged for making available the neutron beam time.

- ¹R. von Helmolt, J. Wecker, B. Holzapfel, L. Schultz, and K. Samwer, *Phys. Rev. Lett.* **71**, 2331 (1993); Y. Tomioka, A. Asamitsu, Y. Moritomo, H. Kuwahara, and Y. Tokura, *ibid.* **25**, 5108 (1995); P. Schiffer, A. P. Ramirez, W. Bao, and S. W. Cheong, *ibid.* **18**, 3336 (1995); B. Raveau, A. Maignan, and V. Caignaert, *J. Solid State Chem.* **114**, 297 (1995).
- ²C. Zener, *Phys. Rev.* **81**, 440 (1951); P. de Gennes, *ibid.* **118**, 141 (1960).
- ³H. Y. Hwang *et al.*, *Phys. Rev. Lett.* **75**, 914 (1995); R. Havinga, *Philips J. Res.* **21**, 432 (1996).
- ⁴J. Fontcuberta *et al.*, *Phys. Rev. Lett.* **76**, 1122 (1996).
- ⁵R. D. Shannon, *Acta Crystallogr. Sec. A* **32**, 751 (1976).
- ⁶N. Furukawa, *J. Phys. Soc. Jpn.* **63**, 3214 (1994).
- ⁷J. Inoue and S. Maekawa, *Phys. Rev. Lett.* **74**, 3407 (1995).
- ⁸A. J. Millis, B. I. Shraiman, and R. Mueller (unpublished).
- ⁹J. M. De Teresa *et al.*, *Phys. Rev. Lett.* **76**, 3392 (1996).
- ¹⁰J. B. Goodenough, *Mater. Res. Bull.* **6**, 967 (1971); *Phys. Rev.* **164**, 785 (1967); M. Takano *et al.*, *Phys. Rev. Lett.* **67**, 3267 (1991).
- ¹¹J. M. D. Coey, M. Viret, L. Ranno, and K. Ounadjela, *Phys. Rev. Lett.* **75**, 3910 (1995); M. F. Hundley, M. Hawley, R. H. Heffner, Q. X. Jia, J. J. Neumeier, J. Tesmer, J. D. Thompson, and X. D. Wu, *Appl. Phys. Lett.* **67**, 860 (1995).
- ¹²K. Knížek *et al.*, *J. Solid State Chem.* **100**, 292 (1992).